

Synthesis and structural and magnetic characterisation of copper(II) complexes of mixed phosphonate-antimonate ligands†

Shoaib Ali, Christopher A. Muryn, Floriana Tuna and Richard E. P. Winpenny*

Received 7th July 2009, Accepted 24th October 2009

First published as an Advance Article on the web 20th November 2009

DOI: 10.1039/b913467k

A polynucleating oxygen donor ligand based on condensation of *p*-chlorophenylstibonic acid (ArSbO₃H₂) and *t*-butylphosphonic acid is reported. [(SbAr)₂O(HO₃P^tBu)₆] contains two antimony centres, bridged by an oxide and two hydrogen phosphonates. Reaction with copper acetate under solvothermal conditions produces four new polymetallic copper complexes. With pyridine used as a base the major product is a tetracopper cage, [Cu₄O₂(SbAr)₂(O₃P^tBu)₂(O₂CMe)₂(OMe)₆], with the four copper centres arranged in a rhombus; a minor product is a tricopper complex, [Cu₃O₄(SbAr)₂(O₃P^tBu)₄(py)₃]. With LiOMe as base the major product is again the tetranuclear cage, but the minor product is a heterometallic cage, [Cu₅Li₄O₆(SbAr)₄(O₃P^tBu)₆(O₂CMe)₂(OMe)₄(MeOH)₄]. With 2,6-lutidine as base an octametallc complex is formed, [Cu₈O₄(SbAr)₂(O₃P^tBu)₆(O₂CMe)₄(lutidine)₂]. Magnetic studies show both anti-ferromagnetic and weak ferromagnetic exchange between the copper centres in these new complexes.

Introduction

A number of groups have been examining the use of phosphonate ligands to make polymetallic cage complexes. Our work in this area was originally inspired by a paper by Kingsley and Chandrasekhar, who showed that phosphonates could be used as bridging ligands to make a large copper(II) cage, with pyrazoles as co-ligands.¹ Using this approach we have made a number of cobalt,² nickel³ and vanadium cages.⁴ We also examined the reaction of phosphonates with pre-formed carboxylate cage compounds, producing new cages with iron⁵ and manganese.⁶ This reaction, where carboxylates are displaced by phosphonates causing growth of the cage complex due to the greater denticity of the phosphonate ligand, has been pursued with great success by Konar and Clearfield,⁷ and a number of other groups.⁸ Both tactics are used to avoid the insolubility of metal phosphonates which had previously restricted their uses in making cage complexes, with a much greater prevalence of phosphonates being used in making 2D-materials.⁹

To extend this work we examined antimonates as possible ligands, and found polycondensation products which suggest antimonates could be used as inorganic cryptands.¹⁰ As no condensation is observed for phosphonates, and polycondensation is found for antimonates we reasoned that mixing phosphonic acids and stibonic acids might lead to partial condensation and polydentate oxygen donor ligands. We reported a preliminary communication on this subject recently, and the resulting cobalt(II) complexes.¹¹ Main group phosphonates have been studied for a number of years by Roesky¹² and others,¹³ but not, to our knowledge, used as ligands for transition metals. Here we report

an investigation of the coordination chemistry of copper(II) with one of these phosphonate-antimonate ligands.

Experimental

Preparation of compounds

All reagents, metal salts and ligands were used as obtained from Aldrich. Analytical data were obtained by the microanalytical service of the University of Manchester and are given in Table 1.

[(SbAr)₂O(HO₃P^tBu)₆] **1**

p-Chlorophenylstibonic acid (ArSbO₃H₂) (0.4 g, 1.4 mmol) and *t*-butylphosphonic acid 0.43 g (2.8 mmol) were added to MeCN (20 ml) and the mixture was stirred for 24 h. It was then filtered and filtrate was allowed to crystallise by slow evaporation. Crystals of **1** formed after one week. Yield: 60%.

[Cu₄O₂(SbAr)₂(O₃P^tBu)₂(O₂CMe)₂(OMe)₆] **2**

Compound **1** (0.13 g, 0.10 mmol) and copper acetate (0.08 g, 0.40 mmol) were added to methanol (6 mL) and pyridine (0.1 mL) in a Parr digestion bomb. The bomb was sealed and heated at 100 °C for 12 h and then cooled slowly. Blue crystals of **2** were obtained directly from the reaction. Yield: 40%

[Cu₃O₄(SbAr)₂(O₃P^tBu)₄(py)₃] **3**

The same procedure was followed as for **2**. The crystals of **2** were removed, and the blue solution remaining was filtered and allowed to evaporate slowly. Blue crystals of **3** were formed after several days. Yield: 30%

[Cu₅Li₄O₆(SbAr)₄(O₃P^tBu)₆(O₂CMe)₂(OMe)₄(MeOH)₄] **4**

Compound **1** (0.13 g, 0.10 mmol) and copper acetate (0.08 g, 0.40 mmol) were added to methanol (6 mL) and LiOMe (0.023 g,

School of Chemistry, The University of Manchester, Oxford Road, Manchester, UK M13 9PL. E-mail: richard.winpenny@manchester.ac.uk; Fax: +44-161-275-4616

† CCDC reference numbers 739330–739333. For crystallographic data in CIF or other electronic format see DOI: 10.1039/b913467k

Table 1 Analytical data for compounds 1–5

Compound	Formula	Analytical data ^a					
		C	H	Cu	N	P	Sb
1	C ₃₆ H ₇₂ Cl ₂ O ₁₉ P ₆ Sb ₂	33.72 (33.03)	4.89 (5.54)	—	—	13.40 (14.19)	18.06 (18.60)
2	C ₃₀ H ₅₀ Cl ₂ Cu ₄ O ₁₈ P ₂ Sb ₂	26.80 (27.10)	3.72 (3.79)	17.77 (19.12)	—	3.81 (4.66)	19.20 (18.31)
3	C ₄₃ H ₅₉ Cl ₂ Cu ₃ N ₃ O ₁₆ P ₄ Sb ₂	33.05 (34.36)	4.19 (3.95)	11.41 (12.68)	2.62 (2.79)	7.70 (8.24)	14.90 (16.20)
4 ^b	C ₆₀ H ₁₀₄ Cl ₄ Cu ₅ Li ₄ O ₃₆ P ₆ Sb ₄	25.97 (28.43)	3.66 (4.31)	11.45 (12.02)	—	6.84 (7.10)	17.95 (18.48)
5	C ₅₈ H ₉₂ Cl ₂ Cu ₈ N ₂ O ₃₀ P ₆ Sb ₂	29.96 (30.20)	3.90 (4.02)	21.88 (22.04)	1.31 (1.21)	7.32 (8.05)	10.66 (10.56)

^a Found (calc). ^b Also measured: Li 0.97(1.07).

Table 2 Crystal data for compounds 1–5

Compound	1	2	3	4	5
Formula	C ₃₆ H ₆₂ Cl ₂ O ₁₉ P ₆ Sb ₂	C ₃₀ H ₅₀ Cl ₂ Cu ₄ O ₁₈ P ₂ Sb ₂	C ₄₃ H ₆₇ Cl ₂ Cu ₃ N ₃ O ₁₉ P ₄ Sb ₂	C ₆₁ H ₁₀₄ Cl ₄ Cu ₅ Li ₄ O ₃₇ P ₆ Sb ₄ ·C _{0.26} H _{1.08} O _{0.71}	C ₅₈ H ₉₂ Cl ₂ Cu ₈ N ₂ O ₃₀ P ₆ Sb ₂
M _r	1299.08	1329.20	1582.92	2605.19	2305.88
Crystal system	Triclinic	Monoclinic	Triclinic	Triclinic	Monoclinic
Space group	P $\bar{1}$	P2 ₁ /n	P $\bar{1}$	P $\bar{1}$	P2 ₁ /n
a/Å	10.4506(19)	13.2383(4)	11.6323(2)	14.1112(3)	4.3110(3)
b/Å	11.6444(18)	11.1442(3)	13.2236(4)	15.8788(3)	21.4852(4)
c/Å	22.684(3)	15.5501(4)	21.2764(6)	23.7777(5)	14.3972(3)
α (°)	94.982(13)	90.00	91.158(2)	92.306(2)	90.00
β (°)	99.542(14)	99.411(3)	102.161(2)	92.089(2)	103.040(2)
γ (°)	90.679(13)	90.00	104.612(2)	110.555(2)	90.00
V/Å ³	2711.0 (8)	2263.23(11)	3086.51(14)	4977.32(18)	4312.62(15)
Crystal size/mm		0.30 × 0.20 × 0.20	0.30 × 0.20 × 0.20	0.35 × 0.30 × 0.20	0.30 × 0.20 × 0.15
ρ _c /g cm ⁻³	1.591	1.951	1.703	1.743	1.776
Crystal shape and colour	colourless block	blue block	green block	green block	blue block
Total reflns	29942	15153	26149	47395	31096
ind.reflns/R int	9551/0.0604	4603/0.0179	12539/0.0270	20218	8773
reflns with I > 2σ(I)	5296	4066	9374	14707	7067
Parameters	604	269	719	1229	500
restraints	0	0	0	656	0
R ₁ , wR ₂	0.0547, 0.1259	0.0209, 0.0524	0.0285, 0.0666	0.0444, 0.0968	0.0296, 0.0724
goodness of fit	0.95	1.094	0.993	1.021	1.054
largest residuals/e Å ⁻³	2.45	0.66	0.87	2.62	1.13

Common features: Z = 2; T = 100(2) K; radiation = Mo-Kα, λ = 0.71073 Å

0.6 mmol) in a Parr digestion bomb. The bomb was sealed and heated at 100° C for 12 h and then cooled slowly. The blue solution was filtered and coloured crystals of **4** were obtained by slow evaporation of the filtrate. Yield: 5%.

[Cu₈O₄(SbAr)₂(O₃PⁱBu)₆(O₂CMe)₄(lutidine)₂] **5**

Compound **1** (0.13 g, 0.10 mmol) and copper acetate (0.08 g, 0.40 mmol) were added to MeCN (6 mL) and 2,6-lutidine (0.1 mL) in a Parr digestion bomb. The bomb was sealed and heated at 100° C for 12 h and then cooled slowly. Blue crystals of **5** were obtained directly from the reaction. Yield: 35%.

Structure determinations

Data were collected on a Oxford Xcalibur CCD diffractometer (Mo-Kα, λ = 0.71069 Å). In all cases the selected crystals were mounted on the tip of a glass pin using Paratone-N oil and placed in the cold flow (100 K) produced with an Oxford Cryocooling device.¹¹ Complete hemispheres of data were collected using ω-scans (0.3°, 30 s/frame). Integrated intensities were obtained with SAINT+¹² and they were corrected for absorption using

SADABS.¹² Structure solution and refinement was performed with the SHELX-package.¹² The structures were solved by direct methods and completed by iterative cycles of ΔF syntheses and full-matrix least-squares refinement against F². Crystal data are given in Table 2.

Magnetic measurements

The magnetic properties of polycrystalline samples were investigated in the temperature range 2–300 K, by using a Quantum Design MPMS XL SQUID magnetometer equipped with a 7 T magnet. Magnetic susceptibility data were corrected for the diamagnetism of the compounds by using Pascal constants and for the diamagnetic contribution of the sample holder by measurement.

Results

Compound **1** is made straightforwardly from mixing *p*-chlorophenylstibonic acid (ArSbO₃H₂) and *t*-butylphosphonic acid together in MeCN with a 1 : 2 mole ratio. The crystal structure (Fig. 1) shows two Sb centres bridged by a μ₂-oxide and two

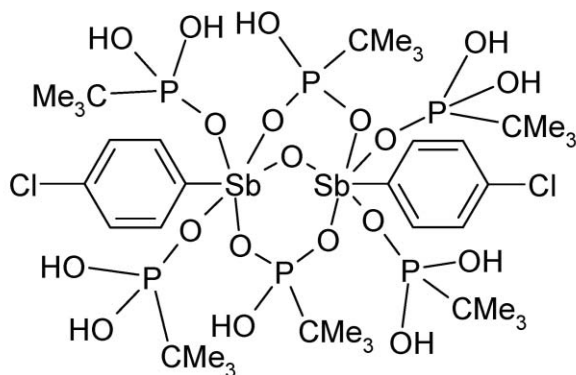
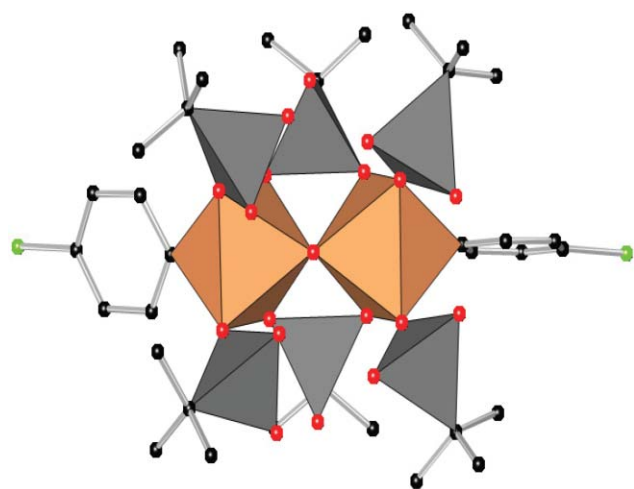


Fig. 1 The structure of **1** in the crystal showing as a polyhedral view. Colour code: Sb, orange; P, gray; O, red; C, black; Cl, green. A line drawing of the structure is shown below.

hydrogen phosphonate ligands. Four further hydrogen phosphonates are attached to the Sb centres. The Sb–O bond lengths involving the μ_2 -oxide are 1.931(5) and 1.944(5) Å, while the Sb–O bonds involving the phosphonates are in the range 1.982(5)–2.034(5) Å.

Compound **2** was obtained by the reaction of **1** with copper acetate in MeOH under solvothermal conditions, using pyridine as base. The crystals of **2** appeared directly upon slow cooling of the MeOH solution. The structure is centro-symmetric and contains four Cu centres arranged in a rhombus (Fig. 2). Selected bond distances and bond angles for **2** are given in Table 3. The Cu1...Cu2 edge of the rhombus is bridged by a μ_3 -oxide (O5) which is also attached to the Sb1 site. This Cu...Cu contact on this edge is 3.50 Å. Cu1 is bridged to Cu2a centre by two oxygens (O1a and O2) from phosphonates and by an acetate group; this leads to a Cu...Cu distance of 3.01 Å. There are also four μ_2 -methoxides in the structure, bridging Cu...Sb contacts.

Both copper sites have square pyramidal geometry; for each O5, an oxygen from an acetate, and oxygen from a phosphonate and an O-atom from the μ_2 -methoxide occupy equatorial positions. The axial position is occupied by an oxygen from a phosphonate; O2 for Cu1 and O1 for Cu2. All the equatorial bond distances are around 2.0 Å, while the axial Cu(1)–O(2) bond distance is

Table 3 Selected bond lengths (Å) and angles (°) in compound **2**

Cu1–O5	1.8971(17)	Cu1–O9	1.9197(17)
Cu1–O1	1.9534(17)	Cu1–O7	2.0155(17)
Cu1–O2	2.3813(16)	Cu2–O5	1.8977(17)
Cu2–O8	1.9177(17)	Cu2–O2	1.9571(16)
Cu2–O4	2.0111(17)	Cu2–O1	2.3563(16)
O5–Cu1–O9	168.95(7)	O5–Cu2–O8	169.26(7)
O5–Cu1–O1	93.25(7)	O5–Cu2–O2	93.78(7)
O9–Cu1–O1	94.99(7)	O8–Cu2–O2	93.62(7)
O5–Cu1–O7	78.90(7)	O5–Cu2–O4	79.11(7)
O9–Cu1–O7	92.63(7)	O8–Cu2–O4	93.06(7)
O1–Cu1–O7	172.04(7)	O2–Cu2–O4	172.39(7)
O5–Cu1–O2	94.05(6)	O5–Cu2–O1	94.61(6)
O9–Cu1–O2	93.73(7)	O8–Cu2–O1	93.46(7)
O1–Cu1–O2	86.92(6)	O2–Cu2–O1	87.54(6)
O7–Cu1–O2	94.87(6)	O4–Cu2–O1	95.68(6)
Cu1–O1–Cu2	87.98(6)	Cu1–O2–Cu2	87.19(6)
Cu1–O5–Cu2	134.77(9)		

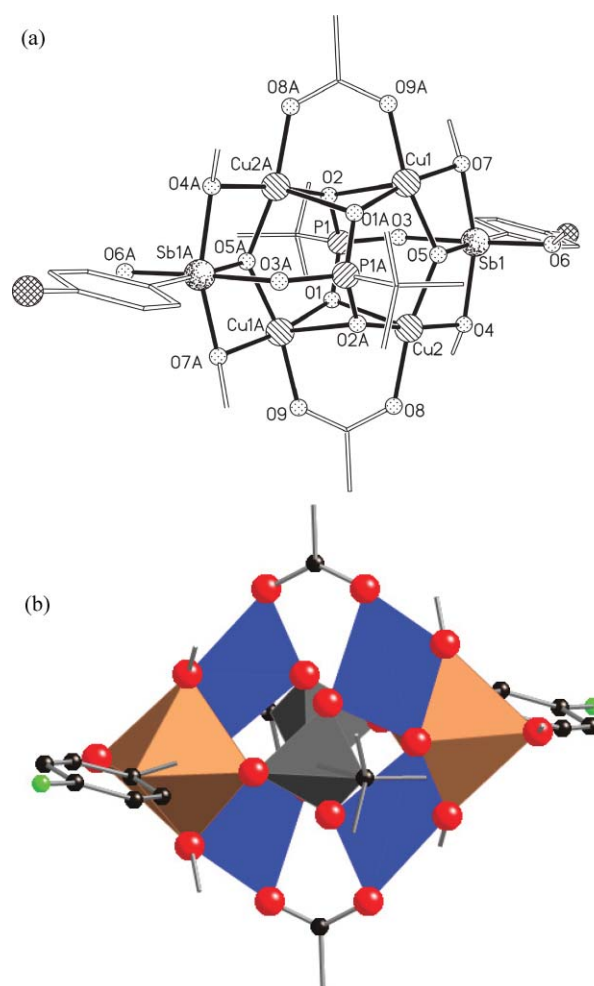


Fig. 2 The structure of **2** in the crystal shown (a) as a ball-and-stick view (aryl group on Sb excluded for clarity), and (b) as a polyhedral view. Colour scheme as Fig. 1, plus Cu, blue polyhedra.

2.3813(16) Å. All the bond angles are as expected for a square pyramid.

The two symmetry-equivalent Sb centres, are six co-ordinate and attached to one terminal methoxide (O6), two μ -methoxides (O4 and O7), one μ_3 -oxide (O5) and one oxygen (O3) from a phosphonate. The Sb–O bond distances again depend on the type

of oxygen involved; the shortest bond is to O5 at 1.950(2) Å; bonds to methoxide fall in the range 1.962–2.045(2) Å, while those to phosphonate are longest at 2.084(2) Å. The bonding mode for both of the phosphonates is 5.221, with the mononucleating O-donor bound to antimony. The same product, with almost the same yield and purity was obtained by using LiOMe, NaOMe, KOMe or lutidine as a base instead of pyridine. Therefore changing base in this reaction does not change the major product obtained, however the by-products are different, with **3** obtained if pyridine is used and **4** if LiOMe is used.

Compound **3** was obtained by slow evaporation of the mother liquor after crystals of **2** were collected. The molecular structure of compound **3** is shown in Fig. 3. The structure contains two Sb and three Cu centres occupying the corners of a square pyramid. The two Sb centres are connected through a μ_2 -oxide (O4) and a μ_3 -oxide (O6), with Sb–O bond distance of around 2.0 Å. The Cu1 and Cu3 sites have square pyramidal geometry with two oxygen donors from phosphonates (O14 and O15 for Cu1, O10 and O12 for Cu3), a μ_2 -oxide (O1 or O5) and an N-donor from pyridine in equatorial positions, while a μ_2 -oxide (O19) occupies the axial position of each copper site. All the equatorial bond distances around these copper centres are in the range of 1.91–2.00 Å, while the axial Cu1–O19 bond distance is 2.527(2) Å. The bond angles are as expected for a square pyramid. The Cu2 site has a trigonal bipyramidal coordination geometry in which one pyridyl ligand and a μ_3 -oxide (O6) occupy the axial positions while three oxygen donors from phosphonates, (O7, O11, and O16), occupy the equatorial positions of the trigonal bipyramid. All the equatorial bond distances around Cu(2) centre are 1.9–2.1 Å, while the axial bond distances are around 1.9 Å. There is no trend in the Sb–O bond lengths which fall in the range 1.971(2)–2.045(2) Å. The phosphonates show two bonding modes; three, involving P1, P2 and P3, show the 3.111 mode while the fourth bridges Cu1 and Cu3 using the 2.110 mode. The inter atomic distance between Cu(1) and Cu(3) centres is 4.18 Å. The selected bond distances and bond angles for compound **3** are shown in Table 4.

Compound **4** was obtained by the reaction of **1** with copper acetate in MeOH under solvothermal conditions, using LiOMe as base. Crystals of **2** are the major product of the reaction, and form on slow cooling of the solution within the bomb. Crystals of **4** appeared by slow evaporation of the MeOH solution after

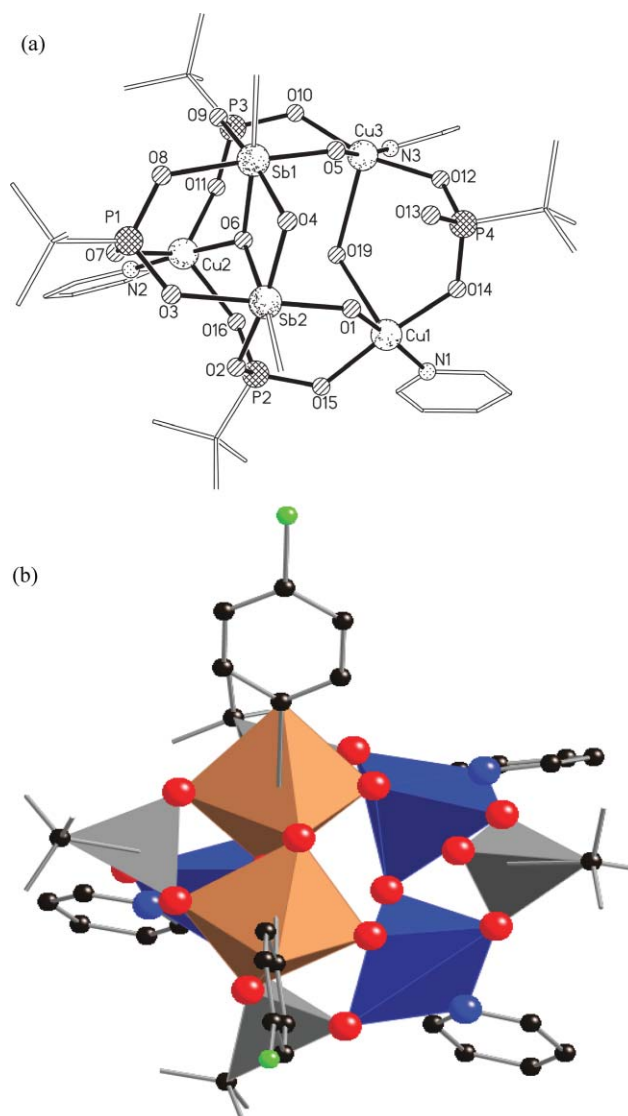


Fig. 3 The structure of **3** in the crystal shown (a) as a ball-and-stick view (aryl group on Sb excluded for clarity), and (b) as a polyhedral view. Colour scheme as Fig. 2, plus N, blue spheres.

crystals of **2** were removed. The low yield of **4** prevented magnetic characterisation.

The structure of **4** (Fig. 4) contains five Cu and four Sb centres connected through six phosphonates, two acetates and four methoxides. The copper centres make a bow-tie consisting of two triangles (Cu1, Cu2 and Cu3, and Cu3, Cu4 and Cu5 respectively) connected at Cu3. There is one Sb centre above and one below the plane of each triangle. Thus Sb1 and Sb2 lie above and below the first triangle while Sb3 and Sb4 are associated with the second triangle.

Four of the copper sites, Cu1, Cu2, Cu4 and Cu5, have square pyramidal geometries, while Cu3 is square planar. The Cu1 centre has one μ_3 -oxide (O16), a μ_2 -methoxide (O17), an oxygen from an acetate (O10) and an oxygen (O9) from a phosphonate at equatorial positions of the square pyramid, while a further phosphonate oxygen (O31) occupies the equatorial position. All the equatorial bond distances are around 1.95 Å, while the axial Cu1–O31 bond distance is 2.390(4) Å. The O10–Cu1–O31 bond

Table 4 Selected bond lengths (Å) and angles (°) in compound **3**

Cu1–O14	1.916(2)	Cu3–O12	1.917(2)
Cu1–O15	1.919(2)	Cu3–O10	1.933(2)
Cu1–O1	2.005(2)	Cu3–O5	2.018(2)
Cu1–N1	2.028(3)	Cu3–N3	2.026(3)
Cu2–N2	1.979(3)	Cu2–O11	2.050(2)
Cu2–O6	1.981(2)	Cu2–O16	2.110(2)
Cu2–O7	1.997(2)		
O14–Cu1–O15	174.70(9)	O12–Cu3–O10	165.67(9)
O14–Cu1–O1	89.86(9)	O12–Cu3–O5	91.00(9)
O15–Cu1–O1	91.77(9)	O10–Cu3–O5	90.49(9)
O14–Cu1–N1	89.01(10)	O12–Cu3–N3	89.13(10)
O15–Cu1–N1	88.37(10)	O10–Cu3–N3	87.42(10)
O1–Cu1–N1	168.35(9)	O5–Cu3–N3	171.93(9)
N2–Cu2–O6	176.24(10)	O7–Cu2–O11	128.77(9)
N2–Cu2–O7	93.16(10)	N2–Cu2–O16	89.05(9)
O6–Cu2–O7	89.92(8)	O6–Cu2–O16	87.31(8)
N2–Cu2–O11	88.69(10)	O7–Cu2–O16	130.73(9)
O6–Cu2–O11	91.07(8)	O11–Cu2–O16	100.47(8)

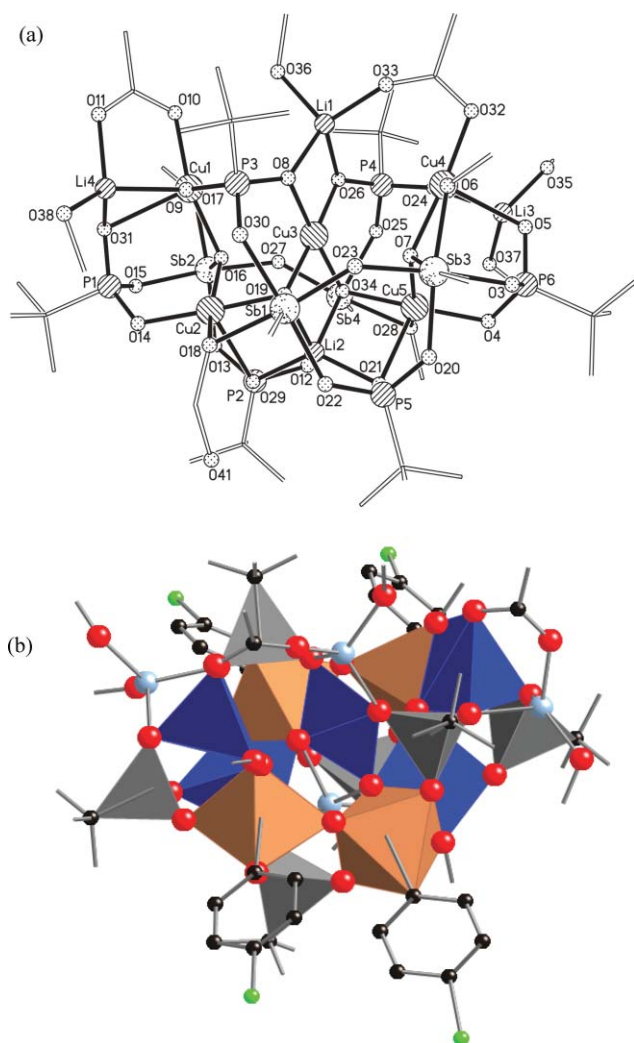


Fig. 4 The structure of **4** in the crystal shown (a) as a ball-and-stick view (aryl group on Sb excluded for clarity), and (b) as a polyhedral view. Colour scheme as Fig. 3, plus Li, light blue spheres.

angle is $104.8(2)^\circ$, causing a distortion in the square pyramidal geometry. The coordination environment around Cu4 involves a similar set of donor atoms.

The Cu2 centre has a μ_3 -oxide (O16), a μ_4 -oxide (O19), a μ_2 -methoxide (O18) and an oxygen (O14) from a phosphonate at the equatorial positions of the square pyramid, while a further oxygen donor (O29) from another phosphonate at the axial site. All the equatorial bond distances are in the range of 1.9–2.0 Å, while axial Cu2–O29 bond distance is 2.401(3) Å. The O14–Cu2–O18 bond angle is $98.7(2)^\circ$ which is the chief distortion in the square pyramidal geometry. The coordination environment around Cu5 involves a similar set of donor atoms to Cu2.

The square planar Cu3 centre is connected to two μ_4 -oxides (O19 and O34) and two phosphonate oxygens (O8 and O26). The Cu3–O bond distances are in the range of 1.92–1.97 Å and all the bond angles are regular. There is a clear trend in the Sb–O bond lengths, with bonds involving oxides falling in the range 1.923–1.961(4) Å, while where phosphonates are involved the Sb–O bonds fall in the range 2.006–2.123(4) Å. Selected bond distances and bond angles for compound **4** are shown in Table 5.

Table 5 Selected bond lengths (Å) and angles ($^\circ$) in compound **4**

Cu1–O10	1.950(4)	Cu4–O32	1.935(4)
Cu1–O16	1.953(3)	Cu4–O7	1.955(3)
Cu1–O17	1.970(4)	Cu4–O6	1.984(4)
Cu1–O9	1.981(4)	Cu4–O24	1.991(4)
Cu1–O31	2.390(4)	Cu4–O5	2.385(4)
Cu2–O14	1.907(3)	Cu5–O4	1.912(3)
Cu2–O16	1.948(4)	Cu5–O34	1.950(3)
Cu2–O19	1.964(3)	Cu5–O7	1.951(3)
Cu2–O18	2.003(4)	Cu5–O28	2.013(3)
Cu2–O29	2.401(3)	Cu5–O21	2.348(4)
Cu3–O19	1.921(3)	Cu3–O26	1.969(4)
Cu3–O34	1.939(3)	Cu3–O8	1.979(3)
Li1–O33	1.884(13)	Li3–O35	1.886(15)
Li1–O8	1.922(12)	Li3–O5	1.919(11)
Li1–O36	1.933(12)	Li3–O37	1.953(13)
Li1–O26	1.990(12)	Li3–O24	1.978(11)
Li2–O29	1.849(9)	Li4–O38	1.879(12)
Li2–O21	1.868(9)	Li4–O31	1.915(12)
Li2–O19	1.967(9)	Li4–O11	1.957(12)
Li2–O34	1.970(9)	Li4–O9	1.969(11)
O10–Cu1–O16	163.97(16)	O32–Cu4–O7	169.70(17)
O10–Cu1–O17	92.53(17)	O32–Cu4–O6	92.10(18)
O16–Cu1–O17	79.29(15)	O7–Cu4–O6	78.93(14)
O10–Cu1–O9	92.62(16)	O32–Cu4–O24	92.32(17)
O16–Cu1–O9	95.48(15)	O7–Cu4–O24	96.32(14)
O17–Cu1–O9	174.77(15)	O6–Cu4–O24	174.24(15)
O10–Cu1–O31	104.77(16)	O32–Cu4–O5	95.74(17)
O16–Cu1–O31	90.03(14)	O7–Cu4–O5	91.19(14)
O17–Cu1–O31	97.24(15)	O6–Cu4–O5	102.47(15)
O9–Cu1–O31	82.34(15)	O24–Cu4–O5	80.76(14)
O14–Cu2–O16	94.18(15)	O4–Cu5–O34	174.78(15)
O14–Cu2–O19	175.15(15)	O4–Cu5–O7	94.48(15)
O16–Cu2–O19	88.23(14)	O34–Cu5–O7	88.51(14)
O14–Cu2–O18	98.68(15)	O4–Cu5–O28	96.84(14)
O16–Cu2–O18	158.64(15)	O34–Cu5–O28	78.78(14)
O19–Cu2–O18	77.80(14)	O7–Cu5–O28	154.91(15)
O14–Cu2–O29	100.67(14)	O4–Cu5–O21	99.33(15)
O16–Cu2–O29	96.00(13)	O34–Cu5–O21	84.39(13)
O19–Cu2–O29	83.23(13)	O7–Cu5–O21	99.00(13)
O18–Cu2–O29	98.28(14)	O28–Cu5–O21	101.15(14)
O19–Cu3–O34	84.73(14)	O19–Cu3–O8	93.52(15)
O19–Cu3–O26	175.35(15)	O34–Cu3–O8	174.93(14)
O34–Cu3–O26	94.17(15)	O26–Cu3–O8	87.95(15)
Cu5–O7–Cu4	116.96(17)	Cu3–O19–Cu2	111.67(16)
Cu2–O16–Cu1	116.02(18)	Cu3–O34–Cu5	110.29(15)

There are four Li centres, each is four coordinate and two of these coordination sites are occupied by oxygen donors from phosphonates, while occupation of the other sites vary. In case of Li1 and Li4, the other two sites are occupied by an oxygen from methanol and a O-atom from acetate. For Li2 centre the two additional sites are occupied by two μ_4 -oxides, while for Li3 two methanol molecules occupy these sites.

The phosphorous centres occupy the triangular faces made by Sb and Cu centres, and then bind further to the external Li atoms. Four of the phosphonates (those involving P1, P2, P5 and P6) have a bonding mode of 4.211, while final two phosphonates (involving P3 and P4) have a 5.221 mode. Each phosphonate, with a bonding mode 4.211, contain one oxygen donor bridging between a Li and a Cu centre while the other two oxygen donors coordinate to either a Sb or Cu centre. Similarly each phosphonate with bonding mode 5.221, has two oxygen donors bridging between Li and Cu centres and one oxygen donor coordinating to an antimony.

Compound **5** was obtained by the reaction of **1** with copper acetate in MeCN under solvothermal conditions, using 2,6-lutidine as base. The crystals of **5** appeared by slow cooling of the

MeCN solution. The structure is centro-symmetric and contains two Sb and eight Cu centres connected through six phosphonates (Fig. 5). The core of the structure is an edge-sharing oxo-centred tetrahedron $\text{Cu}_4\text{Sb}_2(\mu_4\text{-O})_2$; Cu2 and Cu2a are in the shared edge, with Cu3, Cu3a, Sb1 and Sb1a on the exterior vertices. The μ_4 -oxides are O15 and O15a. The three crystallographically unique phosphonates all adopt the 3.111 mode, and bridge edges of this core polyhedron and then on to the additional copper sites. The phosphonate containing P1 bridges from Sb1 to Cu3a (Fig. 5), and then on to Cu1. The phosphonate containing P2 bridges from Sb1 to Cu2, and then to Cu1, while the P3-phosphonate bridges Sb1 to Cu2a and then on to Cu4. There is a μ_3 -oxide between Sb1, Cu3 and Cu4 and there is also a 2.11 bridging acetate between Cu4 and Cu3. The coordination site of Cu1 is completed by a chelating acetate while that of Cu4 has a terminal lutidine attached.

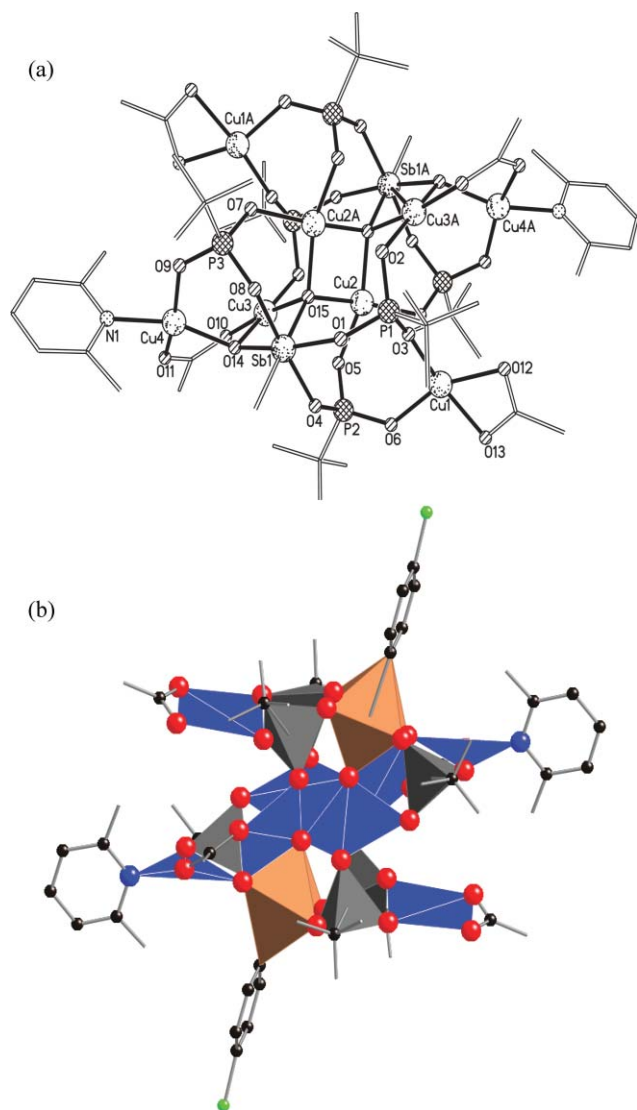


Fig. 5 The structure of **5** in the crystal shown (a) as a ball-and-stick view (aryl group on Sb excluded for clarity), and (b) as a polyhedral view. Colour scheme as Fig. 3.

All the Cu centres are approximately square planar. The Cu1 centre is coordinated to two O-donors from phosphonates (O3 and O6) and the chelating acetate (O12, O13). The chief distortion from

Table 6 Selected bond lengths (Å) and angles (°) in compound **5**

Cu1-O6	1.898(2)	Cu3-O14	1.928(2)
Cu1-O3	1.908(2)	Cu3-O10	1.929(2)
Cu1-O12	1.990(2)	Cu3-O2	1.932(2)
Cu1-O13	2.007(3)	Cu3-O15	2.000(2)
Cu2-O5	1.915(2)	Cu4-O14	1.912(2)
Cu2-O7	1.939(2)	Cu4-O9	1.918(3)
Cu2-O15	1.958(2)	Cu4-O11	1.941(2)
Cu2-O15	2.008(2)	Cu4-N1	1.973(2)
O6-Cu1-O3	98.49(10)	O14-Cu3-O10	93.22(9)
O6-Cu1-O12	157.45(11)	O14-Cu3-O2	171.17(9)
O3-Cu1-O12	99.36(10)	O10-Cu3-O2	95.17(9)
O6-Cu1-O13	93.58(10)	O14-Cu3-O15	80.94(8)
O3-Cu1-O13	159.64(10)	O10-Cu3-O15	172.36(9)
O12-Cu1-O13	65.57(11)	O2-Cu3-O15	90.93(9)
O5-Cu2-O7	95.19(10)	O14-Cu4-O9	99.40(9)
O5-Cu2-O15	160.71(8)	O14-Cu4-O11	89.33(10)
O7-Cu2-O15	99.18(9)	O9-Cu4-O11	161.04(11)
O5-Cu2-O15	87.95(9)	O14-Cu4-N1	159.86(10)
O15-Cu2-O15	82.44(9)	O9-Cu4-N1	87.28(11)
Cu4-O14-Cu3	107.15(10)	O11-Cu4-N1	90.20(11)
Cu2-O15-Cu3a	114.91(10)	Cu2-O15-Cu2a	97.56(9)
		Cu3-O15-Cu2	95.91(9)

square planar geometry is due to the small O12-Cu1-O13 angle (65°) due to the bite angle of acetate. The Cu2 site is coordinated to two μ_4 -oxides (O15 and O15a) and two phosphonate oxygens (O5 and O7a). The Cu3 centre is coordinated to a μ_4 -oxide (O15), a μ_3 -oxide (O14), one oxygen donor (O2) from a phosphonate and one oxygen donor (O10) from acetate. Finally, Cu4 is coordinated to a μ_3 -oxide (O14), one oxygen donor (O9) from a phosphonate, one oxygen donor (O11) from acetate and a lutidine. The Cu–O bond distances are not exceptional. The distances between the Cu centres connected through a μ_4 -oxide (O15) are in the range of 2.97–3.34 Å. The Sb–O bond involving the μ_3 -oxide is 1.962(2) Å, while the other Sb–O bonds in the structure fall in the range 1.998–2.022(2) Å. Selected bond distances and bond angles for compound **5** are shown in Table 6.

In each case it is necessary to make compound **1** prior to reacting with the copper salt. If the components that make **1** are added separately to a copper salt, then insoluble and uncharacterisable materials form, which we believe are polymeric copper phosphonates. The condensation reaction to give **1** restricts the formation of these polymeric materials.

Magnetic studies

DC magnetic studies were carried out on polycrystalline samples of **2**, **3** and **5**, in the temperature range 2–300 K. The temperature dependence of the magnetic susceptibility of **2** is shown as a $\chi_m T$ vs. T plot (χ_m = molar magnetic susceptibility) in Fig. 6. The product $\chi_m T$ is $1.42 \text{ cm}^3 \text{ K mol}^{-1}$ at room temperature and decreases rapidly upon cooling to approach $0.012 \text{ cm}^3 \text{ K mol}^{-1}$ at 1.8 K. In addition, the magnetic susceptibility curve shows a maximum at *ca.* 145 K, which is the signature of dominant antiferromagnetic exchange between metal centers leading to a $S = 0$ ground state. The non-zero value of the $\chi_m T$ at low temperatures is probably due to both temperature independent paramagnetism (TIP) and a small amount of paramagnetic impurity (approximately 1.5%). Similar behaviour has been reported for other Cu(II) tetramers.¹⁴

In compound **2** the four copper centres are arranged in a rhombus with the super-exchange paths along alternate edges of the rhombus very different. For two edges the exchange is *via*

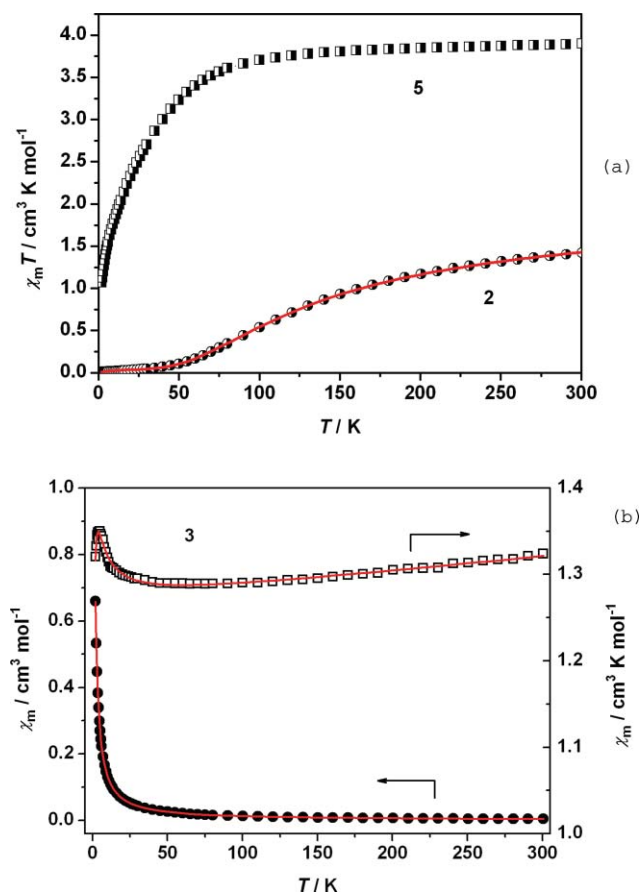


Fig. 6 a) Plots of $\chi_m T$ vs. T for compounds **2** and **5**, with best fit of the data for **2** shown as a solid line; b) Plots of χ_m and $\chi_m T$ vs. T for compound **3** with the best fit of the data shown as a solid line.

two O-atoms from phosphonates and a 2.11-bridging carboxylate, while on the other two edges the bridging is *via* a μ_3 -oxide, which also binds to a Sb centre.

Attempts to simulate the magnetic data of **2** on the base of the general spin Hamiltonian $H = -J_a(S_1S_2 + S_3S_4) - J_b(S_2S_3 + S_1S_4) - J_c(S_1S_3 + S_2S_4)$ with $S_1 = S_2 = S_3 = S_4 = 1/2$ failed, because the three exchange couplings are correlated and could not be determined unambiguously. Setting any one of the exchange coupling constants to zero also failed to fit the data. However, with J_b and J_c fixed to zero, and taking into account a small percentage of paramagnetic impurity (*ca.* 1.2%) - assumed to be a copper(II) monomer with a similar g factor - the data could be fitted reasonably well giving $J_a = -164.2 \text{ cm}^{-1}$ and $g = 2.17$; this g value is very close to the value of 2.173 determined by EPR spectroscopy. This suggests that the magnetic exchange along one edge of the rhombus is much larger than any other exchange interaction present, so we assumed that the magnetic behaviour of **2** could also be modeled as two weakly-interacting copper(II) dimers, and used eqn (1) to fit the data.

$$\chi_m^{Cu_4} = \frac{4N\beta^2 g^2}{k_B(T - \theta)} \frac{1}{3 + \exp(-J/k_B T)} (1 - \rho) + \rho \frac{N\beta^2 g^2}{k_B T} + TIP \quad (1)$$

A Weiss constant, θ , was included to take into account possible exchange interaction between dimers. The best fit was obtained

with $g = 2.166$, $J = -165.4 \text{ cm}^{-1}$, $\theta = -1.93 \text{ K}$, with the paramagnetic impurity fraction $\rho = 0.015$, $TIP = 240 \times 10^{-6} \text{ cm}^3 \text{ mol}^{-1}$ and $R = 1.0 \times 10^5$ (R is the reliability factor defined as $\sum_i [(\chi_m T)_{\text{obs}}(i) - (\chi_m T)_{\text{calc}}(i)]^2 / \sum_i [(\chi_m T)_{\text{obs}}(i)]^2$).

The fit is excellent (solid line, Fig. 6a), but this fit does not define the edge of the rhombus that corresponds to the stronger antiferromagnetic exchange. Taking into account the structure of this compound, it is reasonably to assume that the stronger magnetic exchange occurs *via* the μ_3 oxide bridge as the bridging angle at this oxygen is most obtuse ($\text{Cu1-O5-Cu2} = 135^\circ$). The other edge is bridged by an acetate ligand, and two μ_2 -oxygen atoms from phosphonate. The position of these two phosphonate oxygens is such that they are in an axial position on one Cu and an equatorial position on the second; such bridging makes the magnetic orbitals orthogonal and would lead to a weak, and possibly weakly ferromagnetic, exchange interaction.¹⁵

For compound **3** the room temperature value of $\chi_m T$ is $1.32 \text{ cm}^3 \text{ K mol}^{-1}$, above the calculated value of $1.24 \text{ cm}^3 \text{ K mol}^{-1}$ for three $S = 1/2$ centers with $g = 2.1$ (Fig. 6b). The value declines slowly on cooling to reach $1.29 \text{ cm}^3 \text{ K mol}^{-1}$ at 50 K, before increasing to $1.35 \text{ cm}^3 \text{ K mol}^{-1}$ at 5 K. Below 5 K, $\chi_m T$ decreases again and reaches $1.32 \text{ cm}^3 \text{ K mol}^{-1}$ at 2 K. Close inspection of the structure of **3** shows that the Cu2 center is well isolated from the other two coppers, Cu1 and Cu3, so that we can model the magnetic behaviour of **3** as the sum of contributions of a Cu(II) dimer and a Cu(II) monomer, using eqn (2). A Weiss constant θ was incorporated into analysis to take account of weak intermolecular interactions that occur at low temperatures. Any interaction between the mono-copper centre and the dimer is also contributing to this number. The best fit of χ_m , as well as of $\chi_m T$, using eqn (2), gave $g = 2.12$, $J = 5.15 \text{ cm}^{-1}$, $\theta = -0.3 \text{ K}$, with $R = 6.58 \times 10^{-6}$ and $TIP = 180 \times 10^{-6} \text{ cm}^3 \text{ K mol}^{-1}$.

$$\chi_m^{Cu_3} = \frac{2N\beta^2 g^2}{k_B(T - \theta)} \frac{1}{3 + \exp(-J/k_B T)} + \frac{N\beta^2 g^2}{4k_B(T - \theta)} + TIP \quad (2)$$

The results show that the magnetic interaction between Cu1 and Cu3 is ferromagnetic ($J = 5.15 \text{ cm}^{-1}$), and this can be rationalized as arising from the orthogonality of the magnetic orbitals of square-planar copper(II) centers ($d_{x^2-y^2}$ orbitals) and bridging oxygen atoms (p orbitals) along the Cu1-O19-Cu3 connection. The second bridging ligand that connect Cu1 and Cu3 is a phosphonate group disposed in equatorial-equatorial position with respect to the adjacent copper ions. This ligand may promote antiferromagnetic exchange, but exchange coupling through phosphonate ligands is normally found to be small.⁶

The magnetic susceptibility data of **5** are plotted as $\chi_m T$ against T in Fig. 6a. The room temperature $\chi_m T$ value of $3.89 \text{ cm}^3 \text{ K mol}^{-1}$ indicates that any interaction between the metal centres is weak. Below 100 K, $\chi_m T$ falls steadily which suggests that the predominant interactions in the cage are *anti*-ferromagnetic. The value of $\chi_m T$ at 2 K is $1.07 \text{ cm}^3 \text{ K mol}^{-1}$; $\chi_m T$ is still falling it seems likely that the ground state of the cage is $S = 0$. Given the low symmetry of the cage with many possible exchange paths, no attempt to fit this data was made.

Conclusion

Compound **1** is clearly a pro-ligand that can be combined with copper(II) to produce new polymetallic complexes, with

the nuclearity of the complex dependent on the base used in the reaction. Initial magnetic studies show *anti*-ferromagnetic or weak ferromagnetic exchange between the spin centres in these compounds.

Acknowledgements

SA thanks the Higher Education Commission of Pakistan for a studentship, and REPW thanks the Royal Society for a Wolfson Merit Award. This work was supported by the EPSRC(UK).

References

- (a) V. Chandrasekhar and S. Kingsley, S., *Angew. Chem., Int. Ed.*, 2000, **39**, 2320–2322; (b) V. Chandrasekhar, L. Nagarajan, R. Clérac, S. Ghosh and S. Verma, *Inorg. Chem.*, 2008, **47**, 1067–1073; (c) V. Chandrasekhar, P. Sasikumar, R. Boomishankar and G. Anantharaman, *Inorg. Chem.*, 2006, **45**, 3344–3351; (d) V. Chandrasekhar, L. Nagarajan, R. Clérac, S. Ghosh, T. Senapati and S. Verma, *Inorg. Chem.*, 2008, **47**, 5347–5354.
- (a) E. K. Brechin, R. A. Coxall, A. Parkin, S. Parsons, P. A. Tasker and R. E. P. Winpenny, *Angew. Chem., Int. Ed.*, 2001, **40**, 2700–2703; (b) S. Langley, M. Helliwell, R. Sessoli, S. J. Teat and R. E. P. Winpenny, *Inorg. Chem.*, 2008, **47**, 497–507; (c) S. Langley, M. Helliwell, R. Sessoli, S. J. Teat and R. E. P. Winpenny, *Dalton Trans.*, 2009, 3102–3110.
- B. A. Breeze, M. Shanmugam, F. Tuna and R. E. P. Winpenny, *Chem. Commun.*, 2007, 5185–5187.
- (a) S. Khanra, M. Kloth, H. Mansaray, C. A. Muryn, F. Tuna, E. C. Sañudo, M. Helliwell, E. J. L. McInnes and R. E. P. Winpenny, *Angew. Chem., Int. Ed.*, 2007, **46**, 5568–5571; (b) S. Khanra, M. Helliwell, F. Tuna, E. J. L. McInnes and R. E. P. Winpenny, *J. Mol. Struct.*, 2008, **890**, 157–162.
- (a) E. I. Tolis, M. Helliwell, S. Langley, J. Raftery and R. E. P. Winpenny, *Angew. Chem., Int. Ed.*, 2003, **42**, 3804; (b) S. Khanra, S. Konar, A. Clearfield, M. Helliwell, E. J. L. McInnes, E. Tolis, F. Tuna and R. E. P. Winpenny, *Inorg. Chem.*, 2009, **48**, 5338–5349; (c) S. Khanra, M. Helliwell, F. Tuna, E. J. L. McInnes and R. E. P. Winpenny, *Dalton Trans.*, 2009, 6166–6174.
- (a) M. Maheswaran, G. Chastanet, S. J. Teat, T. Mallah, R. Sessoli, W. Wernsdorfer and R. E. P. Winpenny, *Angew. Chem., Int. Ed.*, 2005, **44**, 5044–5048; (b) M. Shanmugam, G. Chastanet, T. Mallah, R. Sessoli, S. J. Teat, G. A. Timco and R. E. P. Winpenny, *Chem.–Eur. J.*, 2006, **12**, 8777–8785; (c) M. Shanmugam, M. Shanmugam, G. Chastanet, R. Sessoli, T. Mallah, W. Wernsdorfer and R. E. P. Winpenny, *J. Mater. Chem.*, 2006, **16**, 2576–2578.
- S. Konar, N. Bhuvanesh and A. Clearfield, *J. Am. Chem. Soc.*, 2006, **128**, 9604–9605; (a) S. Konar and A. Clearfield, *Inorg. Chem.*, 2008, **47**, 3492–3494; (b) S. Konar and A. Clearfield, *Inorg. Chem.*, 2008, **47**, 3489–3491; (c) S. Konar and A. Clearfield, *Inorg. Chem.*, 2008, **47**, 5573–5579.
- (a) Y.-S. Ma, Y. Song, Y.-Z. Li and L.-M. Zheng, *Inorg. Chem.*, 2007, **46**, 5459–5461; (b) R. Murugavel, N. Gogoi, K. G. Suresh, S. Lavek and H. C. Verma, *Chem.–Asian J.*, 2009, **4**, 923–935.
- (a) A. Clearfield, *Prog. Inorg. Chem.*, 1997, **47**, 371–510; (b) D.M. Poojary, B. Zhang and A. Clearfield, *J. Am. Chem. Soc.*, 1997, **119**, 12550–12559; (c) C. V. Krishnamohan Sharma and A. Clearfield, *J. Am. Chem. Soc.*, 2000, **122**, 4394–4402; (d) D. Kong, J. Zoň, J. McBee and A. Clearfield, *Inorg. Chem.*, 2006, **45**, 977–986.
- V. Baskar, M. Shanmugam, M. Helliwell, S. J. Teat and R. E. P. Winpenny, *J. Am. Chem. Soc.*, 2007, **129**, 3042–3043.
- S. Ali, V. Baskar, C. A. Muryn and R. E. P. Winpenny, *Chem. Commun.*, 2008, 6375–6377.
- (a) Y. Yang, H.-G. Schmidt, M. Noltemeyer, J. Pinkas and H. W. Roesky, *J. Chem. Soc., Dalton Trans.*, 1996, 3609–3610; (b) M. G. Walawalkar, R. Murugavel, H. W. Roesky and H.-G. Schmidt, *Organometallics*, 1997, **16**, 516–518; (c) M. G. Walawalkar, R. Murugavel, H. W. Roesky, I. Usón and R. Kraetzner, *Inorg. Chem.*, 1998, **37**, 473–478; (d) Y. Yang, J. Pinkas, M. Schafer and H. W. Roesky, *Angew. Chem., Int. Ed.*, 1998, **37**, 2650–2653; (e) Y. Yang, J. Pinkas, M. Noltemeyer, H.-G. Schmidt and H. W. Roesky, *Angew. Chem., Int. Ed.*, 1999, **38**, 664–666.
- (a) V. Chandrasekhar and K. Gopal, *Appl. Organomet. Chem.*, 2005, **19**, 429–436; (b) M. R. Mason, *J. Cluster Sci.*, 1998, **9**, 1–23; (c) R. Murugavel and S. Shanmugam, *Chem. Commun.*, 2007, 1257–1259.
- (a) L. Merz and W. Haase, *J. Chem. Soc., Dalton Trans.*, 1978, 1594; (b) A. Bencini, D. Gatteschi, C. Zanchini, J. G. Haasnoot, R. Prins and J. Reedijk, *J. Am. Chem. Soc.*, 1987, **109**, 2926; (c) R. Wegner, M. Gottschaldt, H. Görls, E.-G. Jäger and D. Klemm, *Chem.–Eur. J.*, 2001, **7**, 2143.
- O. Kahn, *Molecular Magnetism*, VCH Publisher, New York, 1993p 26.